A Practical Copper Loss Measurement Method for the Planar Transformer in High-Frequency Switching Converters

Yongtao Han, *Student Member, IEEE*, Wilson Eberle, *Senior Member, IEEE*, and Yan-Fei Liu, *Senior Member, IEEE*

***Abstract*—In this paper, a new and practical measurement method is proposed to characterize the planar transformer copper loss operating in a high-frequency switching mode power supply (SMPS). The scheme is easy to set up, and it provides an equivalent winding alternating current resistance, which is the result of all the field effects on the transformer windings to achieve more accurate copper loss characterization. A detailed error analysis for the proposed copper loss measurement method is conducted. The analysis results can provide useful guidelines on the SMPS transformer copper loss measurement scheme design. Measurement results on the copper loss of a planar transformer in a high-frequency dc/dc converter are presented. In order to verify the measurement results, a time-domain finite-element analysis transient solver is adopted to analyze the transformer copper loss. Good matching between the simulation and measurement results is achieved.**

***Index Terms*—Copper loss, finite-element analysis (FEA), planar transformer, pulsewidth modulation (PWM), switching mode power supply (SMPS), winding ac resistance.**

I. Introduction

PLANAR magnetic components are widely used in high-switching-frequency power converters [1]–[5]. At higher frequencies, the magnetic losses in the switching mode power converters have also been increased. Accurate analysis and characterization of the transformer core loss and copper loss play an important role in the design and optimization of switching mode power supplies (SMPSs). The characterization for the transformer core loss has been frequently discussed in the literature [6]–[9]. However, little work has been done on the transformer copper loss characterization under the actual operating condition. This paper focuses on the characterization of the transformer copper loss for high-frequency SMPSs, and a new measurement method is proposed.

Analytical and measurement methods are usually used to obtain the transformer copper loss in SMPSs. The analytical method is based on Fourier series analysis [10]–[14]. With this method, the pulsewidth-modulated (PWM) current waveform flowing through the SMPS transformer windings is decomposed into $i_{\rm dc}$, if any, and the harmonics as $i_1, i_2, \ldots$; then, the transformer winding dc resistance $(R_{\rm dc})$ is calculated, and the ac resistance under each harmonic $(R_1, R_2, \ldots)$ is obtained using Dowell's results [15] for the primary and secondary windings, respectively. The transformer total copper loss is then calculated as

$$\begin{aligned} P_{\rm copper} &= P_{\rm pri} + P_{\rm sec} \\ &= \left(R_{\text{dc-pri}} \cdot I_{\text{dc-pri}}^2 + \frac{1}{2} \sum_{n=1}^{N} I_{n\text{-pri}}^2 \cdot R_{n\text{-pri}} \right) \\ &\quad + \left(R_{\text{dc-sec}} \cdot I_{\text{dc-sec}}^2 + \frac{1}{2} \sum_{n=1}^{N} I_{n\text{-sec}}^2 \cdot R_{n\text{-sec}} \right). \end{aligned} \tag{1}$$

The analytical method can only be applied to simple transformer structures, and rough approximations on the core and winding structure are always made. Because of this limitation, they cannot handle complicated winding structures, especially with parallel windings. Another drawback is that they cannot take into account the effect of the nonideal field distributions within the transformer, such as the fringing flux, bypass flux, and winding edge effect [16]–[19]. These effects will impact the winding copper loss significantly, especially for a planar transformer.

The measurement method is widely used to obtain the transformer copper loss and, at the same time, verify the analytical method results. Compared with the analytical method, the measurement method has potentially higher accuracy because it could theoretically include all the field effects on the windings within the transformer structure. However, delicate equipment and experiment are usually needed. In addition, no scheme is available to measure the transformer copper loss under the actual operating conditions, such as directly using the PWM current waveforms.

In this paper, after reviewing the limitations of the existing transformer copper loss measurement methods, a new scheme is proposed to measure the transformer copper loss operating in high-frequency SMPSs. An equivalent winding ac resistance for each winding is measured under the transformer's actual operating condition, which is the result of all the field effects on the winding to achieve an accurate copper loss result, including the nonideal field distributions and field interaction between the primary and secondary windings. The scheme is easy to set up.

Manuscript received October 8, 2005; revised February 4, 2007.

Y. Han was with the Department of Electrical and Computer Engineering, Queen's University at Kingston, Kingston, ON K7L 3N6, Canada. He is now with Jabil Circuit Inc., Shanghai 200233, China.

W. Eberle and Y.-F. Liu are with the Department of Electrical and Computer Engineering, Queen's University at Kingston, Kingston, ON K7L 3N6, Canada (e-mail: yanfei.liu@queensu.ca).

Color versions of one or more of the figures in this paper are available online at http://ieeexplore.ieee.org.

Digital Object Identifier 10.1109/TIE.2007.899877

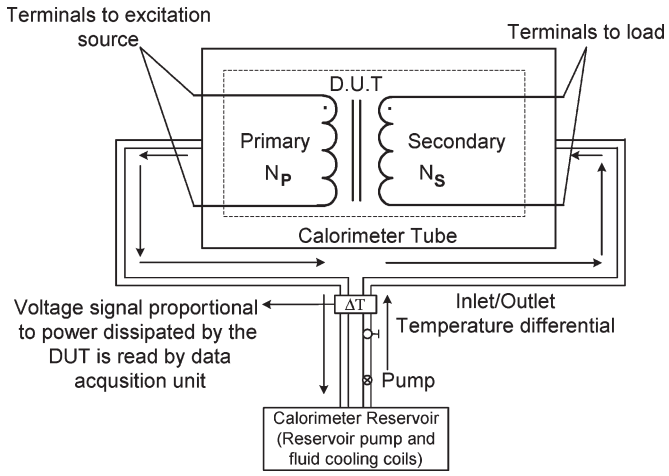

Fig. 1. Calorimeter method for transformer winding copper loss measurement.

It also avoids the difficulties that are encountered by other measurement methods, such as the separation of core loss from copper loss.

Section II reviews the existing copper loss measurement methods and highlights their drawbacks. In Section III, the new copper loss measurement method is proposed with the detailed explanations on the measurement principle, the important issues, and the proposed key steps that are related to the measurement. Section IV provides the measurement results on a planar transformer winding ac resistances using the proposed method. The measurement results are compared with the finite-element analysis (FEA) simulation results by a time-domain transient solver. In Section V, measurement is conducted to demonstrate the impact of the field interaction between the primary and secondary windings on the winding ac resistances, which is ignored by the existing measurement methods. The results show that the proposed method can provide more accurate copper loss information because it can include the field interaction between windings. Section VI performs the error analysis on the proposed measurement method and demonstrates that the proposed method can achieve measurement accuracy higher than 5%. Section VII provides the conclusion.

II. Review of Existing Transformer Copper Loss Measurement Methods

Two measurement methods are commonly used to measure the transformer copper loss, namely, 1) the calorimetric method and 2) the Fourier-analysis-based method.

A. Calorimetric Method

The calorimetric method is a typical indirect method and is widely used in the transformer winding copper loss measurement for SMPSs. One of the schemes is shown in Fig. 1. The measurement principle of this scheme is stated as follows: The transformer under test is placed in the calorimeter tube, which is enclosed in a near-adiabatic chamber in order to minimize the heat loss in the system. The flow within the tube is maintained at a constant rate with the pump and control valve. The reservoir and the cooling coils are used to maintain the constant temperature for the inlet tube fluid. The "ΔT" block is a thermocouple pile, which measures the temperature difference between the inlet and outlet to the calorimeter tube. The transformer copper loss is calculated based on the steady-state temperature rise of a constant flow rate of the calorimeter tube in the chamber.

The calorimetric method can potentially achieve high accuracy in measuring the dissipated power. However, it is very difficult to set up, and a long time is needed to achieve the thermal equilibrium before the experiment can be carried out. Significant leakage inductance and parasitic capacitance are introduced by the terminal leads, which will impact the transformer operation and, hence, reduce the measurement accuracy. Delicate equipment (calorimeter tube and a near-adiabatic chamber) are also needed. One other important drawback is that it cannot distinguish the copper loss from the core loss.

B. Fourier-Analysis-Based Method

Based on Fourier series analysis, several methods have been proposed to characterize the transformer copper loss by measuring the winding ac resistance for each harmonic in the PWM current waveform. In [20], a high-precision multifrequency *LCR* meter is used to measure the transformer winding ac resistance in SMPSs. However, in the measurement, the magnetic core should be removed from the winding to avoid errors. Hence, it cannot reflect the actual field within the transformer and its effects on the winding copper loss. In [21], the authors proposed an analytical method to calculate the transformer winding ac resistance under arbitrary current waveforms. As the verifications on the analytical results, an impedance analyzer is used to measure the transformer winding ac resistance for different harmonic frequencies. Therefore, these methods actually use the sine waveform in the measurement, not directly using the PWM waveform under the transformer winding's actual operating conditions.

It should be noted that, under the transformer's actual operating condition, both the primary and secondary windings are carrying current at the same time. The field interaction between the primary and secondary windings due to the proximity effect has a significant impact on the transformer winding copper loss and is neglected in these methods [22]. With the above methods, the ac resistance of the primary and secondary windings is measured separately, which means that only one winding has current flowing in the measurement. Therefore, another very important disadvantage of these methods is that their results only provide the resistance information for the winding itself and cannot consider the field interaction between transformer windings.

C. Requirements on Transformer Copper Loss Measurement for SMPSs

At high switching frequency, the transformer winding ac resistance significantly increases compared with its dc resistance because of the skin and proximity effects. In addition,

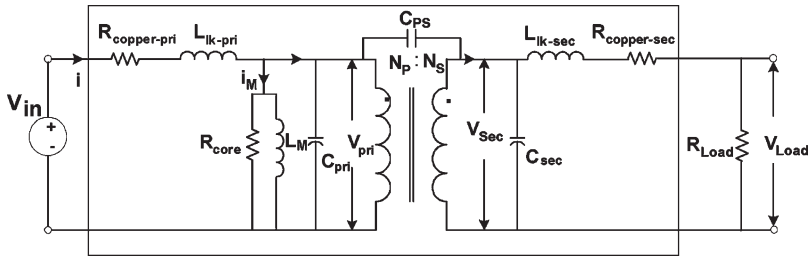

Fig. 2. Equivalent circuit model of a loaded two-winding transformer.

the field interaction between windings and the nonideal field distributions (fringing flux, bypass flux, etc.) within the transformer have significant impact on the winding copper loss. It is also noted that the influence of these factors on the winding ac resistance is strongly structure and frequency dependent. Consequently, these impacts are very difficult to analyze.

Due to the limitations of the analytical methods in calculating the transformer copper loss in high-frequency SMPSs, the measurement method is the preferred way to characterize the transformer copper loss. To avoid the drawbacks of the existing measurement methods in designing the transformer copper loss measurement scheme for SMPSs, the following requirements are important to achieve accurate measurement.

1) "In-Component" Scheme: This means that the ferrite core should not be removed from the windings and the transformer operates in the actual electromagnetic field of the operating conditions. The nonideal field distributions can also be taken into account.

2) Actual PWM Current Waveforms: The PWM current under the transformer's actual operating condition should be directly applied to the windings instead of using the harmonic sinusoidal waveforms.

3) Simultaneous Current Flowing in Both the Primary and Secondary Windings: By achieving this requirement, the field interaction between the primary and secondary windings is included in the copper loss measurement results.

Based on these requirements, a new and "in-component" measurement method is proposed to measure the transformer winding copper loss for SMPSs directly using the PWM current waveforms. This method can provide an equivalent ac resistance for the measurement condition. It considers all the field effects on the windings, including the field interaction between windings, to achieve more accurate results for the copper loss characterization. The transformer copper loss measurement method proposed can be applied to improve the performance of the transformers, as well as the converters, in [23]–[27].

III. Proposed Transformer Copper Loss Measurement Method

In this section, the proposed new transformer copper loss measurement method will be explained in detail. First, some important issues and difficulties in the transformer copper loss measurement are analyzed so that the proposed method can be better understood.

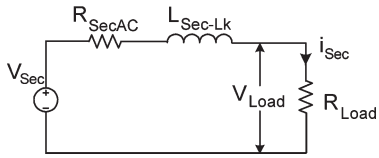

Fig. 3. Secondary side equivalent circuit in the winding ac resistance measurement.

A. Important Issues Related to Copper Loss Measurement

The objective of the transformer copper loss measurement is to obtain an equivalent ac resistance for each winding under the actual operating condition. This equivalent ac resistance can be considered as a characteristic of the winding under the current waveform carried by the winding. In designing the scheme to measure the transformer copper loss in SMPSs, it is important to clarify the following two points:

1) *Current Wave Shape Used in the Measurement:* By analyzing the SMPS circuits, the currents flowing through the transformer windings can be well approximated as rectangular wave shape (unipolar or bipolar) of the corresponding duty ratio by ignoring the small ripple staying on the top [10].
2) *Equivalent AC Resistance:* Although the field interaction between windings has a significant effect on the winding ac resistance, we do not need to separately obtain this information . We only need an equivalent ac resistance of each winding under the operating condition, which considers all the high-frequency effects and field interaction. Then, the total copper loss can be calculated as

$$P_{\text{copper}} = i^2_{\text{PriRMS}} R_{\text{PriAC}} + i^2_{\text{SecRMS}} R_{\text{SecAC}}. \qquad (2)$$

B. Difficulties in Transformer Winding AC Resistance Measurement

The equivalent circuit model of a two-winding transformer under the loaded condition is shown in Fig. 2.

Here, V_{pri} and V_{sec} are the primary and secondary winding voltages; $R_{\text{copper-pri}}$ and $R_{\text{copper-sec}}$ are the primary and secondary winding equivalent resistances; $L_{\text{lk-pri}}$ and $L_{\text{lk-sec}}$ are the primary winding and secondary winding leakage inductances; R_{core} stands for the core loss, and L_{m} is the magnetizing inductance; and C_{ps}, C_{pri}, and C_{sec} are the winding capacitances.

In Fig. 2, $R_{\text{copper-pri}}$ and $R_{\text{copper-sec}}$ are the values that we want to measure, which represent the winding copper loss.

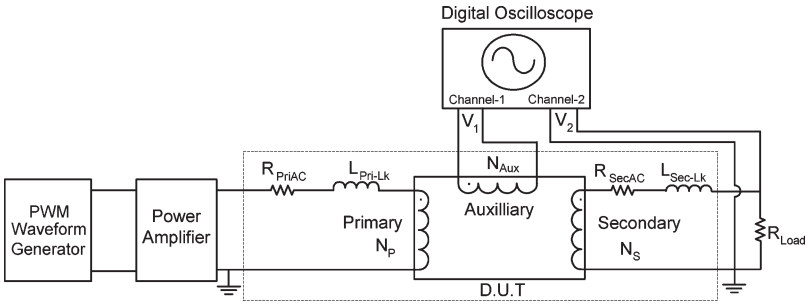

Fig. 4. Transformer winding ac resistance measurement scheme.

It is observed from the equivalent circuit model that the electric circuit components and parameters inside the enclosing rectangular block are all inside the transformer and cannot be accessed by the measurement. Using the secondary side as an example, at the loaded condition, we can derive the secondary-side equivalent circuit as in Fig. 3. (Winding capacitances are ignored because they do not affect the winding resistance calculation).

Only the load voltage $(V_{\rm Load})$ can be measured. Due to the winding resistance and leakage inductance, the actual winding terminal voltage $(V_{\rm Sec})$ is unknown. Although we can calculate the current flowing through the winding ac resistance, which is the same as the current through the load resistor $R_{\rm Load}$, we still cannot obtain the voltage across the winding resistance $R_{\rm SecAC}$ without obtaining the winding terminal voltage $V_{\rm Sec}$. Consequently, the winding ac resistance cannot be measured.

Therefore, it is critical to accurately measure the winding terminal voltage for the winding resistance measurement. In the proposed method, this difficulty is solved by the introduction of an auxiliary winding to accurately measure the terminal voltage of the winding under test.

C. Proposed Copper Loss Measurement Scheme

The proposed transformer winding ac resistance measurement scheme is shown in Fig. 4. Using the secondary winding resistance measurement as an example, the measurement principle is explained as follows.

A PWM waveform generator and a power amplifier are used as the excitation source to provide the rectangular PWM voltage at the primary side. By applying this PWM voltage on the primary side, the magnetic field is established within the transformer, and a PWM voltage is induced at the secondary side. The first requirement (i.e., in-component), as stated in Section II, is satisfied. If a resistive load is connected at the secondary side, a current in rectangular PWM wave shape will flow through the load resistor, as well as the secondary winding equivalent ac resistance, as shown in the equivalent circuit in Fig. 3. Hence, the second condition (i.e., PWM current waveform) stated in Section II is met. Once the secondary side is loaded, current also flows through the primary winding simultaneously. Thus, the third requirement (i.e., simultaneous current flow), as stated in Section II, is also fulfilled.

In order to obtain the secondary winding terminal voltage, an auxiliary winding $(N_{\rm Aux})$ is introduced, as shown in Fig. 4. This winding is an open circuit. Since the same magnetic flux will couple both the secondary winding and the auxiliary winding, the secondary winding terminal voltage $V_{\rm Sec}$ can be calculated by measuring the auxiliary winding terminal voltage $V_{\rm Aux}$ as follows:

$$V_{\rm Sec} = \frac{N_{\rm Sec}}{N_{\rm Aux}} V_{\rm Aux}. \tag{3}$$

The secondary-side current $i_{\rm Sec}$ can be obtained by measuring the voltage across the load resistor. With the winding terminal voltage and the current available, the winding ac resistance $R_{\rm SecAC}$ is calculated as

$$R_{\rm SecAC} = \frac{P_{\rm Sec} - P_{\rm Load}}{I^2_{\rm SecRMS}} \tag{4}$$

where $I_{\rm SecRMS}$ is the rms value of the secondary-side current $i_{\rm Sec}$. $P_{\rm Sec}$ is the power of the secondary winding over one switching period T, which can be calculated as

$$P_{\rm Sec} = \int_0^T V_{\rm Sec} \cdot i_{\rm Sec} \cdot dt = \int_0^T \frac{N_{\rm Sec}}{N_{\rm Aux}} \cdot V_{\rm Aux} \cdot i_{\rm Sec} \cdot dt \tag{5}$$

and $P_{\rm Load}$ is the load resistor power over one switching period, which can be calculated as

$$P_{\rm Load} = \int_0^T V_{\rm Load} \cdot i_{\rm Sec} \cdot dt. \tag{6}$$

The two voltages $V_{\rm aux}$ and $V_{\rm Load}$ (i.e., V_1 and V_2, as shown in Fig. 4, respectively) are measured by a digital oscilloscope (Tektronix TDS 5054 is used in this paper). By calculating the average value of the secondary winding power $P_{\rm Sec}$ and the rms value of the secondary winding current over one switching period using the mathematical functions of the digital oscilloscope, the secondary winding equivalent ac resistance is finally calculated as

$$R_{\text{Sec-AC}} = \frac{P_{\rm Sec} - P_{\rm Load}}{I^2_{\rm SecRMS}} = \frac{\frac{N_{\rm Sec}}{N_{\rm Aux}} \frac{1}{N} \sum_{i=1}^{N} V_{1i} \cdot \frac{V_{2i}}{R_{\rm Load}}}{\frac{1}{N} \sum_{i=1}^{N} \left(\frac{V_{2i}}{R_{\rm Load}} \right)^2} - R_{\rm Load} \tag{7}$$

where

$N_{\rm Sec}$, $N_{\rm Aux}$	turns of the secondary and auxiliary windings;
V_{1i}, V_{2i}	ith sample of the measured voltage values of $V_{\rm aux}$ and $V_{\rm Load}$ by the digital oscilloscope;
N	number of samples in one switching period.

With a less sophisticated digital oscilloscope, the measured raw data can be saved and exported to Excel or MathCad to calculate the winding resistance. In the same way, we can obtain the ac resistance for other secondary windings and the primary winding (i.e., excite the transformer from the secondary side) in the multiwinding transformer.

This scheme is a real "in-component" method and is suitable for multiwinding transformer structures, as the auxiliary winding could be the third winding in the transformer. For a two-winding transformer, an auxiliary winding should be added. This auxiliary winding does not need to carry current. There is no special requirement for this auxiliary winding, and it is easy to do.

This scheme is easy to implement and can include all the field effects on the windings to achieve more accurate measurement for the winding ac resistance and, consequently, the copper loss calculation. It can also avoid the difficulty to separate the core loss from the copper loss. As the digital oscilloscope accomplishes most of the necessary calculations on the measured data, a significant amount of time can be saved on data processing, and measurement result can quickly be obtained.

D. Practical Issues and Key Steps

In order to ensure accurate measurement of the transformer winding ac resistance and eliminate the measurement error from various sources, care should be taken in the test setup and measurement. Practical issues and key steps in the transformer winding ac resistance measurement using the proposed method are explained as follows.

1) Power Source: A PWM waveform generator (Agilent 33120A) and an RF power amplifier are used to provide the PWM voltage source to the transformer. PWM waveforms of different duty ratios are generated. The power amplifier should have enough bandwidth to generate the required waveform.

It is noted that due to the high-frequency effect, the actual winding ac resistor could be different under different operating conditions, such as switching frequency, duty cycle, and amplitude. In order to accurately characterize the transformer winding ac resistance under actual operating conditions, it is always a good idea to use the same PWM current waveform as in the actual condition. Achieving this requirement largely depends on the capability of the power amplifier. The worst case ac resistor happens at the minimum duty cycle and highest current amplitude. Therefore, if the power source cannot provide the required load current, it is suggested to measure the ac resistor at the maximum current that the power source can provide.

2) Load Resistor and Calibration: The load resistor has a large impact on the accuracy of the winding ac resistance measurement result due to its tolerance and its parasitic inductance. In order to minimize the error introduced by the load resistor, it is suggested that a low-inductive resistor be used and the resistor's frequency response be calibrated using an impedance analyzer to obtain the accurate resistance value and phase response. These values can be used in the measurement, calculations, and error analysis.

The following factors are considered in the selection of the load resistor: Because the transformer winding resistance is normally very small, it is a good practice to use a small load resistor. In the measurement setup, low-inductive metal film resistors $(10\% \pm 1\%\ \Omega)$ are connected in parallel to form a small-value load resistor. The parallel method also helps in minimizing the phase shift error that is caused by the parasitic inductance of the resistor and in increasing the total power capability. The frequency response of the resistors is almost flat up to 5 MHz, and it has a small phase angle that changes almost linearly with frequency. In the measurement, the winding excitation voltage is reduced from the nominal input value of the transformer's operating condition in the power converter.

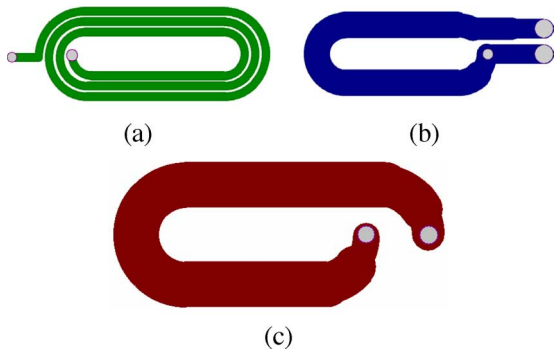

Fig. 5. Planar windings of the transformer used in the paper. (a) PCB track of the primary winding. (b) PCB track of the secondary-I winding. (c) PCB track of the secondary-II winding.

It is important to note that the impedance analyzer only provides small-signal information for the load resistor. The characteristic of the load resistor may be different in a large-signal situation. Our proposed step in calibrating the load resistor is a way to greatly reduce the error that is caused by parasitic inductance and to improve the measurement accuracy. Other better ways to calibrate the load resistor frequency response will further help in improving the measurement accuracy using the proposed method.

3) Calibration on Winding Turns Ratio: The proposed transformer winding ac resistance measurement scheme is a two-port method. The measured winding terminal voltage is obtained from an open-circuit auxiliary winding. Due to the nonperfect magnetic coupling, the parasitic air flux, and the winding terminations, the voltage ratio between the measured winding and auxiliary winding might be different from the corresponding designed integer winding turns ratio. The planar windings in the transformer used in this paper are shown in Fig. 5. It is observed that there is a gap between the winding terminals of the secondary windings. Therefore, some winding turns are not completed, such as for secondary-I winding; some windings extend further outside the core central post, which can be coupled with a parasitic flux, such as for secondary-II winding and for primary winding. These will make the winding terminal voltage ratio between the measured winding and auxiliary winding different from the winding turns ratio. In order to minimize this error, the actual winding turns ratio should be calibrated and be used in the winding resistance measurement and calculation.

Sinusoidal wave is used to calibrate the winding turns ratio, and the result can be used for the PWM waveforms. Sinusoidal excitation is the simplest and easiest waveform in the turns-ratio

calibration for the following reasons: First, it is much easier to obtain a sine waveform; second, no distortions and overshoot will happen to the sine waveform; and third, the definition and calculation of the turns ratio is easy to make, such as using the peak voltage value or peak-to-peak voltage value. It should be noted that the winding turns ratio is the transformer characteristic, and it does not depend on the excitation waveforms.

The procedure of winding turns-ratio calibration is to excite the transformer using a third winding by a sine waveform, and the terminal voltages of the tested and auxiliary windings are measured and the actual turns ratio can be calculated as

$$N_{\text{Turns-Ratio}} = \frac{V_{\text{measured}}}{V_{\text{Aux}}}. \tag{8}$$

The peak voltage value or peak-to-peak voltage value can be used in the calibration. It should be noted that this calibration procedure should be conducted over a range of frequencies in order to cover the frequency range of the PWM harmonics. If the measured winding turns ratios at different frequencies are different, the averaging method can be used to obtain an averaged winding turns-ratio value. When the turns ratio between the measured and auxiliary windings is obtained, it can be used in the winding ac resistance measurement and calculation to achieve more accurate results. By adopting the calibration, the measurement error introduced by the winding turns ratio can be neglected.

4) Averaging Method: In order to eliminate the random error in the measurement, the averaging method is adopted in data processing. The winding ac resistance measurement for each operating condition is repeated for several times (ten times for this paper). Then, these values are averaged by calculation. There will also be the offset error from the power amplifier and the digital oscilloscope in the measurement. This kind of error can be easily eliminated by the offset compensation capability of the digital oscilloscope.

IV. Comparison Between Measurement Results and FEA Simulation

In this section, the transformer winding ac resistance measurement results using the proposed method are presented. As no other method can accurately predict the transformer copper loss under the actual operating condition, the proposed copper loss method is compared with the FEA simulation result using a time-domain solver from ANSOFT [28]. The measurement result and the simulation result are very close to each other.

A. Details of the Transformer Under Test

A high-frequency planar transformer is tested for the winding ac resistance using the proposed scheme. This multiwinding planar transformer is used in an asymmetrical half-bridge (AHB) dc/dc converter with unbalanced secondary windings [29]. In addition to three main power windings, the AHB transformer has three auxiliary windings, one for the control chip power supply and two for driving the secondary-side synchronous rectifiers. The converter schematic and half cross section of the designed transformer are shown in Fig. 6. The

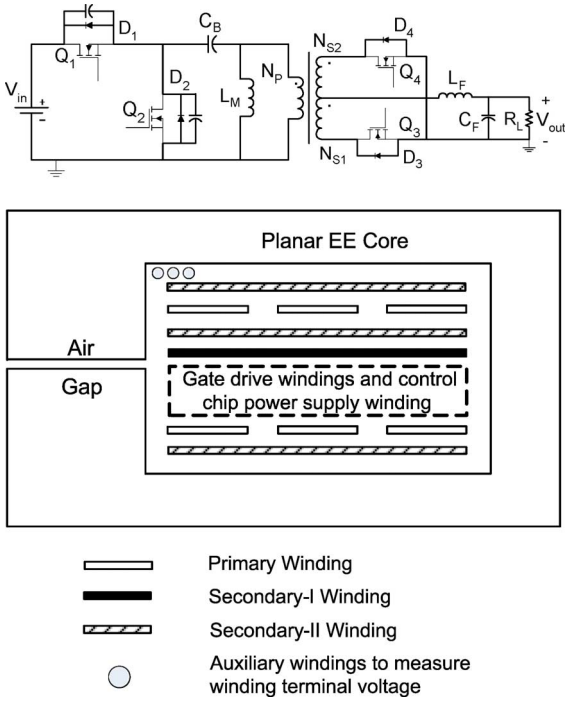

Fig. 6. (top) AHB converter scheme and (bottom) half cross section of the transformer.

dots shown in the figure indicates the added auxiliary winding. The main specifications and parameters of the converter and the transformer are listed as follows:

1) converter input voltage: 35–75 V, nominal at 48 V;
2) converter output: 5 V/25 W;
3) switching frequency: 400 kHz;
4) main winding turns: N_{p}: N_{s1}: $N_{\text{s2}} = 6 : 1 : 3$;
5) core: 41805EC planar core (E18/4/10 in EE combination) of P-material from Magnetics Inc.;
6) winding: 1 oz (35 μm in thickness) copper is used for the winding tracks, producing an eight-layer printed circuit board (PCB).

Fig. 6 also illustrates the placement of the auxiliary windings (shown in dots). The auxiliary winding can be arranged in the gap between the core and the PCB for the planar transformer windings. As this auxiliary winding is only used to measure the winding terminal voltage and it does not carry current, a standard copper wire can be used; and there is no requirement on the wire gauge.

B. FEA Time-Domain Solver

As a powerful tool, the FEA method is widely used in the design and loss analysis for transformers in SMPSs. From the literature, all the work done before is based on the FEA solver using sinusoidal excitations, which is essentially a frequency-domain analysis. In this paper, in order to verify the copper loss measurement results under a real operating condition, a time-domain transient solver in the FEA software package Maxwell from ANSOFT [28] is used to analyze the winding ac resistance. This solver can solve the electromagnetic problems with periodic arbitrary waveform of excitation. The PWM

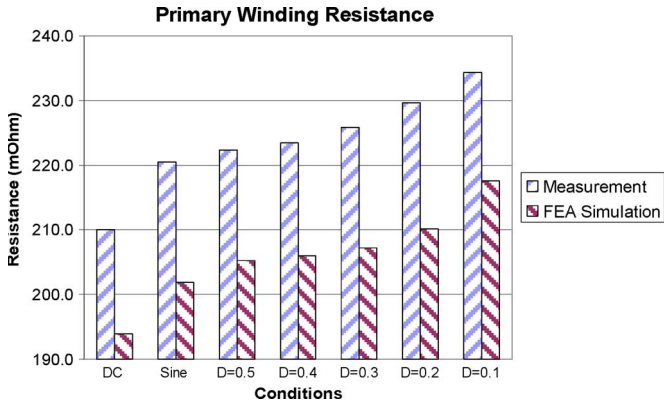

Fig. 7. Measurement and FEA results for the AHB transformer primary winding.

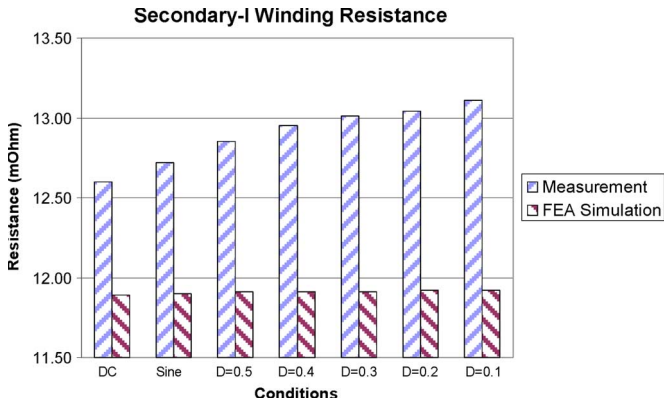

Fig. 8. Measurement and FEA results for the AHB transformer secondary-I winding.

current waveforms flowing in the transformer windings can be directly used as the sources. In addition, 3-D modeling is used to achieve higher accuracy.

It is noted that the following limitations have prevented the wide use of the FEA software package in industry. The first limitation is that this kind of commercial FEA solver software package is very expensive. The second limitation is that extensive time is needed to learn how to use the software to model and analyze the electromagnetic problems. The third and also a very important limitation is that it is very time consuming to carry out the analysis. For example, for analyzing the AHB transformer winding resistance by 3-D modeling, it takes more than 6 h to obtain the copper loss for one operating condition even by using the latest computer.

C. Measurement Results and Comparison for Winding AC Resistance

The ac resistance of the AHB transformer main power windings is measured using the proposed method following the key steps outlined in Section III-D. FEA simulation using the transient solver is conducted to analyze the corresponding ac resistances. In the measurement, as the load resistor, five $10\% \pm 1\%\ \Omega$ metal film resistors are connected in parallel in measuring the primary and secondary-II winding resistances,

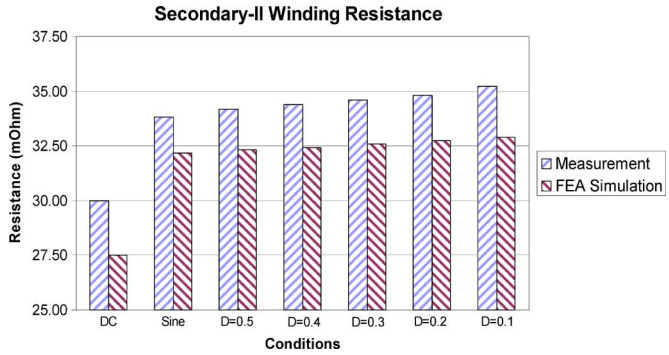

Fig. 9. Measurement and FEA results for the AHB transformer secondary-II winding.

and ten $10\% \pm 1\%\ \Omega$ metal film resistors are connected in parallel in measuring the secondary-I winding resistances.

Figs. 7–9 illustrate the measured results and FEA simulation results for the AHB transformer power windings at 400-kHz bipolar PWM current waveforms of different duty ratios, which correspond to different input voltages of the power converter. Winding dc resistances and the ac resistances at the 400-kHz sine waveform are also provided as reference values.

From the above results, we can observe that the measurement results and FEA simulation results are very close to each other. Using the measurement results as reference values, the difference between the measurement and FEA simulation results is within 8% for all the three AHB transformer power windings. The small difference between them is caused by the measurement and some other factors. First, FEA simulation cannot exactly model the winding structure, even with 3-D modeling. The PCB windings also have certain tolerance in the fabrication. The connection lead for the experiment and the vias and pads of the PCB winding are ignored in the simulation. This can explain why the experimental results are larger than the FEA simulation results. Secondly, the FEA solver also has errors in the solutions.

From both the FEA simulation and measurement results, the following conclusions can be made for the transformer winding resistance.

1) The winding equivalent ac resistance under PWM waveforms is larger than that under the sine waveform of the same frequency.
2) When the duty ratio D decreases (from 0.5 to 0.1), the winding ac resistance increases.

It is noted that the copper PCB tracks used in the transformer winding is 1 oz, or 35 μm thick, which is much smaller than the skin depth of 110 μm at 400 kHz. The winding ac resistance does not change significantly under different operating conditions because the high-frequency eddy current effects do not affect the resistance significantly. It can be expected that the ac resistance will significantly change for different conditions if a thicker copper PCB track (2 or 4 oz) is used as the winding.

In Fig. 10, the oscillograms (auxiliary winding voltage and load resistor voltage) by the digital oscilloscope under different operating conditions in the winding ac resistance measurement are shown for the AHB transformer secondary-I windings. The time interval between the two cursors is one switching period

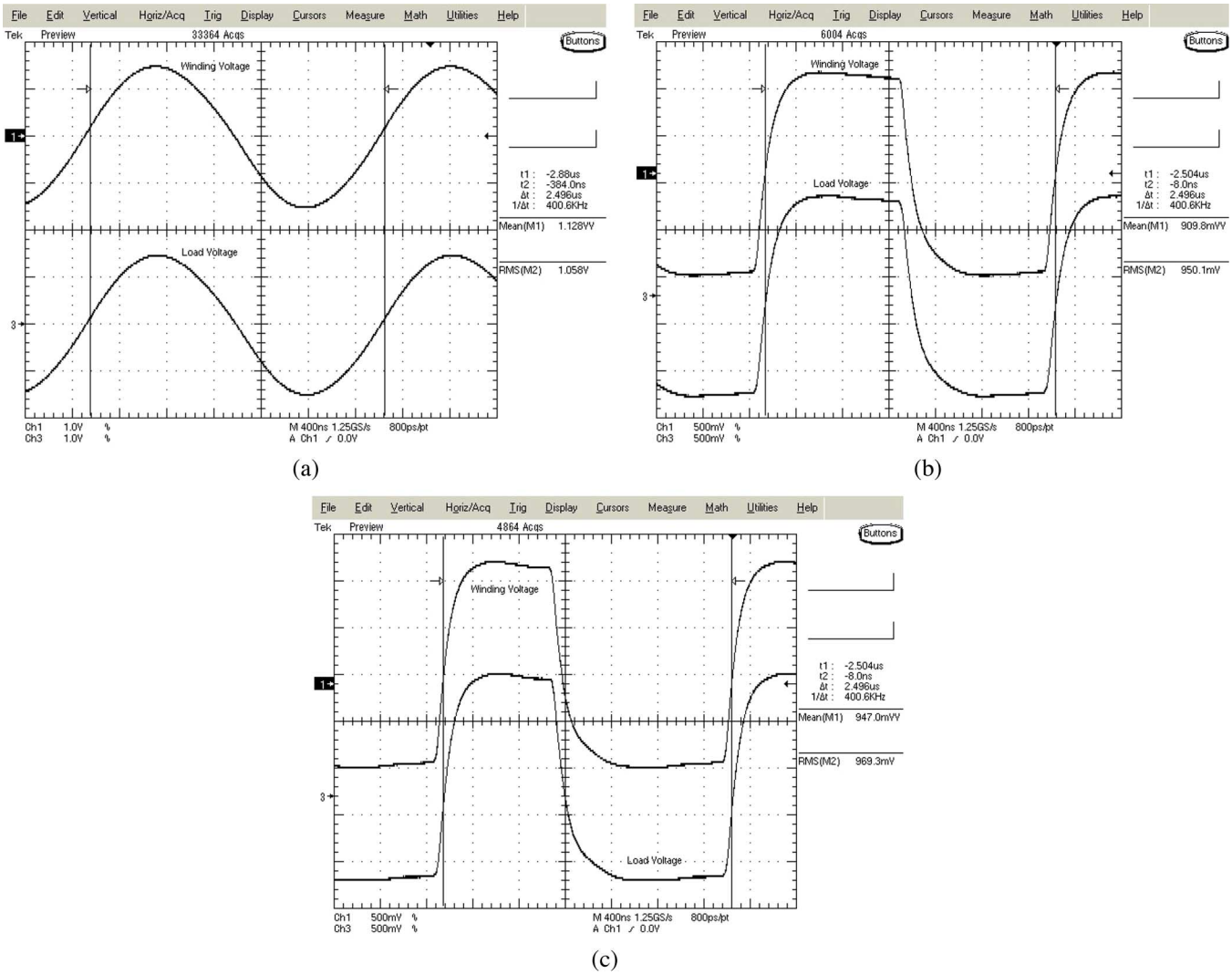

Fig. 10. Secondary-I winding ac resistance measurement waveforms. (a) Sine. (b) $D = 50\%$. (c) $D = 40\%$.

(2.5 μs for 400 kHz). The mathematical functions that are defined in the digital oscilloscope provide the total power of the measured winding and the rms value of the current carried by the winding (also carried by the load resistor). It should be noted that due to limited bandwidth and load capability of the power amplifier, some distortion is observed in the measurement waveforms.

V. Winding Resistance Comparisons: With and Without Field Interaction

As reviewed in Section II, the existing methods for transformer copper loss measurement does not consider the field interaction between primary and secondary windings under the actual operating condition when both windings are carrying current. This will lead to a significant error in the copper loss calculation. In order to show the impact of the field interaction between windings on the winding ac resistance, the AHB transformer winding self-resistance (under the conditions without field interactions between windings) over a range of frequencies (i.e., 1 kHz, 10 kHz, 50 kHz, 100 kHz, 200 kHz, 400 kHz, 800 kHz, and 1 MHz) is measured. Sinusoidal excitations are used. Comparison results show that the field interaction between primary and secondary windings effectively reduces the winding equivalent ac resistance. This is the same conclusion as in [22].

In the measurement, the ferrite core is taken away from the winding in order to avoid the error due to the core loss and avoid the complex parameter extraction from the equivalent circuit model. It should be noted that if the ferrite core is with the windings in the measurement, the winding ac self-resistance should be larger than that without the core due to the nonideal field distributions within the transformer (e.g., the fringing flux for this AHB transformer). FLUKE PM6306 Programmable Automatic *LCR* meter (with accuracy of 5% in measuring resistance larger than 0.1 Ω and accuracy of 10% for resistance between 0.01 and 0.1 Ω) is used in the measurement.

Table I gives the measurement ac resistance values without the field interaction.

Comparing the results in Table I with Figs. 7–9, it is observed that the winding ac resistance values without considering the field interaction are much larger than the resistance values considering the field interaction for all the three windings. For example, under the 400-kHz sine waveform, the primary

TABLE I
AHB TRANSFORMER WINDING AT DIFFERENT FREQUENCIES: WITHOUT FIELD INTERACTION

Frequency (KHz)	1	10	50	100	200
Primary (mΩ)	212	215	220	251	302
Secondary-I (mΩ)	12.6	12.6	12.7	12.7	12.8
Secondary-II (mΩ)	30.0	30.0	31.8	37.0	43.2
Frequency (KHz)	400	600	800	1000	
Primary (mΩ)	371	413	438	454	
Secondary-I (mΩ)	13.1	13.5	14.0	14.5	
Secondary-II (mΩ)	48.6	56.9	63.3	68.2	

winding has an equivalent ac resistance of 221 mΩ when operating in the loaded transformer; its ac resistance without considering the field interaction reaches 371 mΩ, which is 60% higher than when the field interaction is considered. Therefore, a direct application of the winding ac resistance value without considering the field interaction in calculating the transformer total copper loss will lead to significant errors.

VI. ERROR ANALYSIS

In order to ensure that the measurement of the winding ac resistance for the AHB transformer using the proposed method is accurate and valid, it is necessary to identify and analyze the various error sources in the measurement. In this section, the error analysis for the proposed winding ac resistance measurement scheme is separately conducted first, and then the combined loss measurement accuracy is obtained.

As mentioned in Section III-A, the obtained transformer winding ac resistance is a characteristic of the transformer winding under the measurement condition (specific to the amplitude, frequency, and duty ratio of the PWM current waveforms). If the transformer's operating condition (any parameter of the amplitude, frequency, and duty ratio) changes, the measurement and related error analysis should be conducted for the changed condition. Otherwise, measurement accuracy will suffer.

From (7), it is observed that the main error sources in the winding resistance measurement are listed as follows: 1) voltage measurement error; 2) winding turns-ratio error due to the nonperfect magnetic coupling, parasitic coupling flux, and winding termination; 3) tolerance of the load resistor; and 4) time delay introduced into the load current measurement due to the inductance associated with the load resistor. Equation (7) can be rewritten as (using the secondary winding as the example in the derivation)

$$R_{\text{Sec-AC}} = R_{\text{Load}} \cdot \left(\frac{\frac{N_{\text{Sec}}}{N_{\text{Aux}}} \cdot \sum_{i=1}^{N} V_{1i} \cdot V_{2i}}{\sum_{i=1}^{N} (V_{2i})^2} - 1 \right). \quad (9)$$

The effect of each error source on the winding ac resistance measurement is analyzed as follows.

A. Voltage Measurement Error

The TDS5054 digital oscilloscope uses one analog-to-digital converter (ADC) for all the four channels. Hence, the digitizing error that is caused by the ADC in the voltage measurement for each channel can be considered as the same. In the measurement, the auxiliary winding is always selected to be the same turns as the winding under test. Therefore, the same oscilloscope vertical scale can be used for the measurement of the two voltages, and this helps to minimize the resistance measurement error. The digitizing error in the two voltage measurements can be considered as the same. Consequently, the digitizing error will cancel out in the numerator and denominator in the first item of (9). On the other hand, because the sampling number is very large, the random error in the measurement of the digital oscilloscope will be averaged and cancel out each other in the final calculation result. Therefore, it can be assumed that the digitizing error of the digital oscilloscope has no impact on the winding ac resistance measurement and is neglected in the voltage measurement. The averaging method is adopted in data processing. This can further reduce the random error in the measurement.

B. Turns-Ratio Error

An auxiliary winding is used to obtain the winding voltage. The nonperfect magnetic coupling and winding terminations will make the actual winding terminal voltage ratio different from the corresponding turns ratio. The calibration on the winding turns ratio should be carried out to minimize the error, especially when the winding ac resistance is much less than the load resistor. With proper calibration on the winding turns ratio, as described in Section III-D, an actual turns ratio $(N_{\text{Turns-Ratio}})$ is obtained and used in the calculation. This error can then be ignored.

C. Tolerance of Load Resistor

The load resistor used in the measurement has a tolerance of $\pm 1\%$. Theoretically, a relative error of 1% is introduced into the winding ac resistance measurement according to (7).

D. Time-Delay Error

In the load current measurement, a pure resistor value is assumed as the load. However, the inductance of the resistor and the parasitic inductance in the measurement circuit will introduce some time shift error to the current and, consequently, affect the measurement for the total power. This is another important error source in the winding ac resistance measurement.

For SMPSs with the rectangular PWM voltage and current waveform as shown in Fig. 11 (the leakage inductance can be

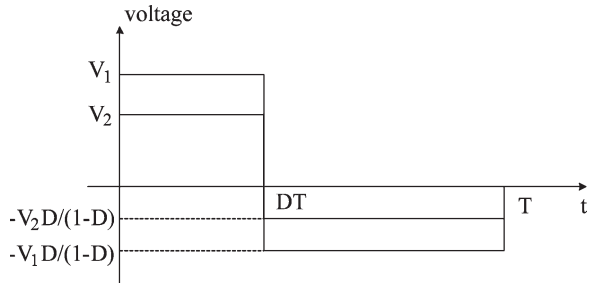

Fig. 11. Typical and ideal PWM voltage and current waveform in measuring winding ac resistance.

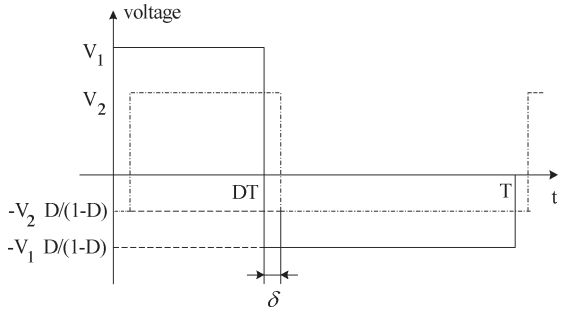

Fig. 12. Time delay introduced into the load current measurement.

neglected for simplification purpose because it is very small), using (9), the winding ac resistance can be calculated as

$$R_{\text{Sec-AC}} = R_{\text{Load}} \cdot \left(N_{\text{Turns-Ratio}} \cdot \frac{V_1}{V_2} - 1 \right). \tag{10}$$

Here,

V_1 positive part amplitude of the auxiliary winding voltage waveform;

V_2 positive part amplitude of the load resistor voltage waveform;

$N_{\text{Turns-Ratio}}$ turns ratio between the auxiliary winding and the measured winding after calibration.

Due to the parasitic inductance, some time delay δ will be introduced into the measurement of the load current, which is obtained by measuring the voltage, as shown in Fig. 12. With this time delay, the winding ac resistance will be (detailed derivation can be found in the Appendix)

$$R_{\text{Sec-AC}} = R_{\text{Load}} \left[N_{\text{Turns-Ratio}} \cdot \frac{V_1}{V_2} \left(1 - \frac{\delta}{D(1-D)T} \right) - 1 \right]. \tag{11}$$

Thus, the relative error due to this time delay is calculated as

$$\frac{\Delta R_{\text{Sec-AC}}}{R_{\text{Sec-AC}}} = \frac{\frac{\delta}{D(1-D)T}}{1 - \frac{V_2}{N_{\text{Turns-Ratio}} \cdot V_1}}. \tag{12}$$

It is related to the time delay, the switching period, the duty ratio of the rectangular PWM waveform, the voltages of the secondary winding, and the load resistor. If the load resistor is much larger than the winding ac resistance, then the ratio of V_2/V_1 in (12) will be very close to "1." In this case, the relative error will be very sensitive to the time delay. A large error will be introduced into the winding ac resistance result. Hence, if a large load resistor (compared with the measured winding ac resistance) is used in the measurement, care should be taken to reduce the time delay caused by the parasitic inductance.

The sources for this time delay δ could be the following: 1) poor frequency response of the load resistor; 2) parasitic inductance in the measurement loop; and 3) trigger jitter and delays for different channels introduced by the oscilloscope. For the digital oscilloscope used in the measurement, the trigger jitter is typical at 8 ps and can be ignored. As the probes for the voltage measurement are originally from the same oscilloscope and match to each other, the phase delay between oscilloscope channels can also be neglected.

TABLE II
RELATIVE ERROR IN MEASURING THE AHB TRANSFORMER PRIMARY WINDING AC RESISTANCE

Conditions	Resistor Tolerance	Time Delay Error	Total
D=0.5	1%	0.2%	1.2%
D=0.3	1%	0.2%	1.2%
D=0.1	1%	0.5%	1.5%

TABLE III
RELATIVE ERROR IN MEASURING THE AHB TRANSFORMER SECONDARY-I WINDING AC RESISTANCE

Conditions	Resistor Tolerance	Time Delay Error	Total
D=0.5	1%	1.3%	2.3%
D=0.3	1%	1.6%	2.6%
D=0.1	1%	3.6%	4.6%

In the measurement setup of this paper, five $10 \pm 1\%\ \Omega$ metal film resistors are in parallel and used as the load resistor in the resistance measurement for the AHB transformer primary and secondary-II windings; ten $10 \pm 1\%\ \Omega$ metal film resistors are in parallel and used in the resistance measurement for the AHB transformer secondary-I winding. The inductance associated with the load resistor is the most important source for the time-delay error. In the experiments, care should be taken to reduce these error sources.

From the measurement results by the impedance analyzer, a phase shift of less than 0.01° is observed for the current sensing resistor at 400 kHz, less than 0.02° at 800 kHz, and 0.05° at 2 MHz. If we use the phase shift at 400 kHz and transfer it to delay time for 400 kHz, the time error can be calculated as

$$\delta = \frac{0.01^\circ}{360^\circ} \times 2.5\ \mu\text{s} = 69.5\ \text{ps}. \tag{13}$$

As the relative error depends on several operation parameters, its value will change for different operating conditions of the transformer. Using the analysis results above, the relative errors in the AHB transformer winding ac resistance measurement are calculated and listed in Tables II–IV.

The error introduced by the load resistor tolerance is 1%. In calculating the time-delay error, the results in (10), (12), and (13) are used. For example, calculation of the time delay

$$R_{\text{Sec-AC}} = R_{\text{Load}} \cdot \frac{N_{\text{Sec}}}{N_{\text{Aux}}} \cdot \frac{V_1}{V_2} \cdot \frac{1}{T} \left[\frac{DT - \delta - \delta\frac{D}{1-D} + \frac{D^2}{(1-D)^2}(T - \delta - DT) - \frac{D}{1-D}\delta}{\frac{D}{1-D}} \right] - R_{\text{Load}}$$
$$= R_{\text{Load}} \cdot \frac{N_{\text{Sec}}}{N_{\text{Aux}}} \cdot \frac{V_1}{V_2} \left[1 - \frac{\delta}{D(1-D)T} \right] - R_{\text{Load}} \tag{A1}$$

TABLE IV
RELATIVE ERROR IN MEASURING THE AHB TRANSFORMER SECONDARY-II WINDING AC RESISTANCE

Conditions	Resistor Tolerance	Time Delay Error	Total
D=0.5	1%	1%	2%
D=0.3	1%	1.2%	2.2%
D=0.1	1%	2.7%	3.7%

in secondary-II winding measurement under 0.5 duty ratio in 400 kHz ($T = 2.5\ \mu$s) is done using the following steps.

Step 1) From (13), we have $\delta = 69.5$ ps.

Step 2) From (10), we can obtain $(N_{\text{Turns-Ratio}} \cdot V_1)/V_2 = 1.0171$ ($R_{\text{Load}} = 2\ \Omega$ and $R_{\text{Sec-AC}} = 34.18\ \text{m}\Omega$ are used in the calculation).

Step 3) Put these results into (12), the time-delay error is calculated as

$$\frac{\Delta R_{\text{Sec-AC}}}{R_{\text{Sec-AC}}} = \frac{\frac{69.5\times10^{-12}}{0.5\times0.5\times2.5\times10^{-6}}}{1 - \frac{1}{1.0171}} = 0.66\% < 1\%. \tag{14}$$

This procedure can be applied to other conditions to obtain the corresponding time-delay error. It is observed that the maximum total relative error is less than 5% for all the three winding resistance measurements.

VII. CONCLUSION

A new measurement method to characterize the transformer copper loss in high-frequency SMPSs is proposed. The proposed measurement method provides an equivalent winding ac resistance under the actual operating condition, which takes into account all the field effects, including the field interaction between windings. Therefore, the measurement provides more accurate copper loss information. The proposed method is easy to set up, and it can also avoid the difficulty of separating the core loss from the copper loss.

Measurement results are presented for a planar transformer operating in a high-frequency PWM dc/dc power converter. Three-dimensional FEA simulation using a time-domain transient solver is used as a comparison. The measured results and simulated results are very close to each other.

A detailed error analysis is given for the proposed winding ac resistance measurement method. The results illustrate that a measurement error of less than 5% can be achieved using the proposed method by following the proposed measurement key steps. It also demonstrates that the proposed schemes can provide accurate characterization for the transformer copper loss in SMPSs. The proposed method can also help in achieving an optimal design of the high-frequency transformer.

APPENDIX
CALCULATION OF THE WINDING AC RESISTANCE WITH THE TIME-DELAY ERROR

From (7) and the waveforms shown in Fig. 12, in calculating the winding ac resistance, the switching period can be divided into four time periods to obtain the total power: $[0, \Delta\delta]$, $[\Delta\delta, DT]$, $[DT, DT + \Delta\delta]$, and $[DT + \Delta\delta, T]$. With the parameter in Fig. 12, we can derive the winding ac resistance as in (A1) (using secondary winding as the example), shown at the top of the page, where

$N_{\text{Sec}}, N_{\text{Aux}}$	turns of the secondary and the auxiliary windings;
V_1, V_2	amplitudes of the positive part of the auxiliary winding voltage and load resistor voltage;
D	duty ratio;
T	switching period;
δ	time delay between the two measured voltages;
R_{Load}	load resistor.

REFERENCES

[1] F. K. Wong, "High frequency transformer for switching mode power supplies," Ph.D. dissertation, Griffith Univ., Brisbane, Australia, Mar. 2004.

[2] N. Dai, "Modeling, analysis, and design of high-frequency, high-density, low-profile transformers," Ph.D. dissertation, VPI&SU, Blacksburg, VA, 1996.

[3] D. van der Linde *et al.*, "Design of a high-frequency planar power transformer in multilayer technology," *IEEE Trans. Ind. Electron.*, vol. 38, no. 2, pp. 135–141, Apr. 1991.

[4] X. Huang, K. D. T. Ngo, and G. E. Bloom, "Design techniques for planar windings with low resistances," in *Proc. IEEE Appl. Power Electron. Conf. and Expo.*, 1995, pp. 533–539.

[5] R. Prieto, O. Garcia, R. Asensi, J. A. Cobos, and J. Uceda, "Optimizing the performance of planar transformers," in *Proc. Appl. Power Electron. Conf. and Expo.*, Mar. 1996, vol. 1, pp. 415–421.

[6] F. D. Tan, J. L. Vollin, and S. M. Cuk, "A practical approach for magnetic core-loss characterization," *IEEE Trans. Power Electron.*, vol. 10, no. 2, pp. 124–129, Mar. 1995.

[7] A. Brockmeyer, "Experimental evaluation of the influence of DC-premagnetization on the properties of the power electronic ferrites," in *Proc. IEEE APEC*, 1996, pp. 454–460.

[8] M. Albach, T. Durbaum, and A. Brockmeyer, "Calculating core loss in transformers for arbitrary magnetizing currents: A comparison of different approaches," in *Proc. IEEE PESC*, 1996, pp. 1463–1468.

[9] J. Li, T. Abdallah, and C. R. Sullivan, "Improved calculation of core loss with nonsinusoidal waveforms," in *Proc. IEEE Ind. Appl. Soc. Annu. Meeting*, 2001, pp. 2203–2210.
[10] P. S. Venkatraman, "Winding Eddy current losses in switching mode power transformers due to rectangular wave currents," in *Proc. POWERCON 11*, Apr. 1984, pp. 1–11. A-1.
[11] A. M. Urling, V. A. Niemela, G. R. Skutt, and T. G. Wilson, "Characterizing high-frequency effects in transformer windings—A guide to several significant articles," in *Proc. APEC*, Mar. 1989, pp. 373–385.
[12] J. A. Ferreira, "Improved analytical modeling of conductive losses in magnetic components," *IEEE Trans. Power Electron.*, vol. 9, no. 1, pp. 127–131, Jan. 1994.
[13] C. R. Sullivan, "Optimal choice for number of strands in a litz-wire transformer winding," *IEEE Trans. Power Electron.*, vol. 14, no. 2, pp. 283–291, Mar. 1999.
[14] J. G. Breslin and W. G. Hurley, "Derivation of optimum winding thickness for duty cycle modulated current waveshapes," in *Proc. 28th Annu. IEEE Power Electron. Spec. Conf.*, 1997, vol. 1, pp. 655–661.
[15] P. L. Dowell, "Effect of eddy currents in transformer windings," *Proc. Inst. Electr. Eng.*, vol. 113, no. 8, pp. 1387–1394, Aug. 1966.
[16] K. D. T. Ngo and M. H. Kuo, "Effects of air gaps on winding loss in high-frequency planar magnetics," in *Proc. Power Electron. Spec. Conf.*, 1988, vol. 2, pp. 1112–1119.
[17] R. Severns, "Additional losses in high frequency magnetics due to non ideal field distributions," in *Proc. IEEE APEC*, 1992, pp. 333–338.
[18] W. Chen, J. He, H. Luo, Y. Hu, and C.-C. Wen, "Winding loss analysis and new air-gap arrangement for high-frequency inductors," in *Proc. IEEE Power Electron. Spec. Conf.*, Jun. 2001, vol. 4, pp. 2084–2089.
[19] K. W. Cheng, Y. Q. Hu, D. H. He, and W. K. Mo, "Effect of geometrical factors on copper loss in high-frequency low-profile transformers," in *Proc. IEEE 31st IAS Annu. Meeting Conf.*, 1996, vol. 3, pp. 1397–1404.
[20] D. K. Conory, G. F. Pierce, and P. R. Troyk, "Measurement techniques for the design of high frequency SMPS transformers," in *Proc. IEEE APEC*, 1988, pp. 341–353.
[21] C. R. Sullivan, "Computationally efficient winding loss calculation with multiple windings, arbitrary waveforms, and two-dimensional or three-dimensional field geometry," *IEEE Trans. Power Electron.*, vol. 16, no. 1, pp. 142–150, Jan. 2001.
[22] J. H. Spreen, "Electrical terminal representation of conductor loss in transformers," *IEEE Trans. Power Electron.*, vol. 5, no. 4, pp. 424–429, Oct. 1990.
[23] G.-B. Koo, G.-W. Moon, and M.-J. Youn, "New zero-voltage-switching phase-shift full-bridge converter with low conduction losses," *IEEE Trans. Ind. Electron.*, vol. 52, no. 1, pp. 228–235, Feb. 2005.
[24] L.-P. Wong, D. K.-W. Cheng, M. H. L. Chow, and Y.-S. Lee, "Interleaved three-phase forward converter using integrated transformer," *IEEE Trans. Ind. Electron.*, vol. 52, no. 5, pp. 1246–1260, Oct. 2005.
[25] B. Choi, W. Lim, S. Bang, and S. Choi, "Small-signal analysis and control design of asymmetrical half-bridge DC–DC converters," *IEEE Trans. Ind. Electron.*, vol. 53, no. 2, pp. 511–520, Apr. 2006.
[26] A. I. Maswood and Z. K. Yoong, "Design aspects of a switch-mode transformer under wide input voltage variation," *IEEE Trans. Ind. Electron.*, vol. 53, no. 3, pp. 752–758, Jun. 2006.
[27] J.-J. Lee and B.-H. Kwon, "DC–DC converter using a multiple-coupled inductor for low output voltages," *IEEE Trans. Ind. Electron.*, vol. 54, no. 1, pp. 467–478, Feb. 2006.
[28] *Maxwell 2D & 3D User's Guide*, ANSOFT Corp., Pittsburgh, PA, 2002.
[29] W. Eberle and Y.-F. Liu, "A zero voltage switching asymmetrical half-bridge DC/DC converter with unbalanced secondary windings for improved bandwidth," in *Proc. IEEE PESC*, 2002, pp. 1829–1834.

Yongtao Han (S'01) received the bachelor's and master's degrees in electrical engineering from Tianjin University, Tianjin, China, in 1993 and 1996, respectively, and the M.Sc. degree in electrical engineering, majoring in power electronics, from Queen's University at Kingston, Kingston, ON, Canada, in December 2003.

After graduation, he became an Electrical Engineer, working in the area of industrial control systems and instruments. In May 2001, he joined the Queen's Power Group, Queen's University. He is currently with Jabil Circuit Inc., Shanghai, China, as an Electronics Engineer. His research interests include high-frequency magnetics and dc/dc and ac/dc switching power supplies.

Wilson Eberle (SM'98) was born in Windsor, ON, Canada. He received the B.Sc. and M.Sc. degrees from Queen's University at Kingston, Kingston, ON, in 2000 and 2003, respectively. He is currently working toward the Ph.D. degree at the Department of Electrical and Computer Engineering, Queen's University at Kingston, under the supervision of Dr. Y.-F. Liu and Dr. P. C. Sen.

From 1997 to 1999, he was an Engineering Co-Op Student at Ford Motor Company, Windsor, ON, for three summers. He has one U.S. patent pending and is the author of 12 technical papers published in conference proceedings and IEEE journals. His research interests include high-efficiency high-power-density low-power dc/dc converters, digital control techniques for dc/dc converters, EMI filter design for switching converters, and resonant gate drive techniques for dc/dc converters.

Mr. Eberle is a recipient of the Ontario Graduate Scholarship and has received awards through the Power Source Manufacturer's Association and Ontario Centres of Excellence to present papers at conferences.

Yan-Fei Liu (S'91–M'94–SM'97) received the B.Sc. and M.Sc. degrees from Zhejiang University, Hangzhou, China, in 1984 and 1987, respectively, and the Ph.D. degree from Queen's University at Kingston, Kingston, ON, Canada, in 1994.

Since August 1999, he has been with the Department of Electrical and Computer Engineering, Queen's University, as an Associate Professor. Prior to this, from February 1994 to July 1999, he was a Technical Advisor at the Advanced Power System Division, Astec (formerly Nortel Networks), where he was responsible for high-quality design, new products, and technology development. His research interests include digital control technologies for dc/dc switching converter and ac/dc converter with power factor correction, EMI filter design methodologies for switching converters, topologies and controls for high switching frequency, low switching loss converters, modeling and analysis of core loss and copper loss for high-frequency planar magnetics, topologies and control for VRM, and large-signal modeling of switching converters.

Dr. Liu received the Golden Apple Teaching Award and Premiere's Research Excellent Award from Queen's University in 2000 and 2001, respectively. He is also the recipient of the "1997 Award in Excellence in Technology" from Nortel.